water

MDPI

Article

Linking Precipitation Deficits to Reservoir Storage: Robust Statistical Analyses in the Monte Cotugno Catchment (Sinni Basin, Italy)

Marco Piccarreta [1,*] and Mario Bentivenga [2]

[1] Ministero dell'Istruzione, dell'Università e della Ricerca Italiana, 00153 Rome, Italy
[2] Department of Basic and Applied Sciences, University of Basilicata, Via Ateneo Lucano 10, 85100 Potenza, Italy; mario.bentivenga@unibas.it
* Correspondence: marco.piccarreta@scuola.istruzione.it

Abstract

This study examines the hydroclimatic controls on reservoir storage dynamics in the Sinni River basin (southern Italy), with a specific focus on the Monte Cotugno dam—the largest earth-fill reservoir in Europe. Using monthly precipitation data (2000–2024) from eight gauges and standardized indicators (SPI at multiple timescales and SRI for storage), we apply robust trend, correlation, autocorrelation, and causality analyses, supported by advanced preprocessing (TFPW), to disentangle climatic influences from anthropogenic pressures. Results show a statistically significant and persistent decline in the SRI series, indicating progressive storage depletion, despite stationary or slightly positive trends in precipitation at annual and hydrologically relevant timescales. These findings highlight the dominant role of cumulative operational losses and systemic inefficiencies—rather than sustained climatic drying—as primary drivers of reservoir decline. Granger causality and lagged-correlation analyses reveal that multi-month to annual precipitation anomalies (SPI-3, SPI-6, SPI-12) exert the strongest influence on storage variations, yet the basin's ability to convert rainfall into effective reservoir supply is severely constrained by infrastructural and management limitations. The study underscores the urgent need to integrate climate-based monitoring with infrastructural modernization and governance reforms to address the combined climatic and anthropogenic pressures increasingly affecting Mediterranean water systems.

Keywords: reservoir storage; Standardized Precipitation Index (SPI); hydrological variability; Granger causality; Mediterranean basin

Academic Editor: David Post

Received: 19 December 2025
Revised: 10 January 2026
Accepted: 12 January 2026
Published: 14 January 2026

1. Introduction

Climate change and population growth are intensifying water scarcity across the Mediterranean region [1], one of the areas most exposed to climate-related risks and high rainfall variability. At present, more than 180 million people in the region are affected by water scarcity, with additional pressures driven by demographic expansion, urbanization, and the intensification of agricultural and tourism activities [2]. The Mediterranean basin hosts approximately 60% of the global population living with less than 1000 m^3 of available freshwater per capita per year, a value well below the globally recognized water-stress threshold [3]. Recent climate projections consistently indicate further declines in precipitation, an increase in the frequency and severity of drought events, and enhanced intra- and inter-annual rainfall variability [4–6]. These climatic pressures, combined with rising

water demand, are expected to lead to more frequent water crises, deterioration of water quality, and significant impacts on agriculture, urban water supply, riverine ecosystems, and marine productivity [7–9].

Dams and large surface reservoirs serve as the primary buffers and regulatory systems for freshwater storage in the Mediterranean, playing a crucial role in mitigating seasonal water deficits and meeting peak demand [10]. However, recent studies show that the regional water crisis has been exacerbated by a considerable reduction in reservoir storage levels, largely attributable to declining precipitation totals and the increasing recurrence of extreme drought episodes [11–13]. Advances in satellite altimetry and remote sensing have enabled the first large-scale, systematic evaluations of these trends, revealing substantial decreases in storage across hundreds of reservoirs worldwide. In many Mediterranean systems, these analyses highlight a chronic inability to reach full capacity under recent adverse climatic conditions.

Within this context, rigorous statistical assessment of the relationship between precipitation and reservoir storage has become essential for developing reliable forecasting tools and for supporting adaptive water-resource planning. Approaches based on standardized precipitation indices (e.g., SPI), correlation and trend analyses, causal inference frameworks, and robust significance tests—capable of accounting for the autocorrelation typical of hydrological time series—now represent key methodologies for quantifying risks, identifying critical thresholds, and improving integrated water-management strategies in the Mediterranean region [14–17].

This study aims to examine, through an innovative and multi-dimensional approach, the relationship between precipitation (at multiple temporal scales, as expressed through the Standardized Precipitation Index, SPI) and stored water resources in the largest earth-fill dam in Europe—the Monte Cotugno Reservoir, a representative system for Mediterranean hydro-climatic conditions. We apply a suite of advanced statistical techniques, including trend analysis, causality assessment, and prewhitening procedures, to disentangle the actual climatic signal from the effects of hydrological memory and anthropogenic trends [18]. The overarching goal is to provide both conceptual and operational tools to support water-resource management in a region facing a high risk of structural water scarcity.

In this framework, the present study adopts a reservoir-centered perspective, focusing on standardized storage dynamics at the scale of a single strategic dam, and complements existing drought assessments by explicitly analyzing how multi-scale precipitation anomalies are transmitted to, or decoupled from, reservoir storage under current hydroclimatic and management conditions. To our knowledge, no previous work has performed a long-term, multi-scale analysis of the SPI–SRI relationship for the Monte Cotugno reservoir, explicitly quantifying lagged cross-correlations, non-stationary behavior and the predictive role of SPI3 and SPI6 for standardized storage. By integrating these climate-based diagnostics with regional evidence on groundwater constraints, structural seepage vulnerabilities and exceptionally high downstream distribution losses, the study offers a novel multi-index framework for understanding why meteorological drought signals do not always translate into proportional changes in reservoir storage in one of the most critical interregional water-supply systems of southern Italy.

2. Study Area

The Monte Cotugno Dam, located in the Basilicata Region near the town of Senise (Province of Potenza), is the largest earth-fill reservoir in Europe and one of the most important water infrastructures in Southern Italy (Figure 1). The dam impounds the Sinni River approximately 33 km upstream of its mouth and about 6 km upstream of the confluence with the Sarmento Creek, intercepting a drainage area of about 804 km^2 out

of the 1290 km^2 total catchment of the Sinni River [19]. Designed for multi-annual water regulation, the reservoir provides an active storage capacity exceeding 430 million m^3 and a maximum capacity of over 500 million m^3. The lake covers an area of approximately 10 km^2, reaches depths greater than 50 m, and is formed by an embankment structure about 1.85 km long and 65 m high at its maximum section. The Monte Cotugno dam was constructed between the early 1970s and the early 1980s, with reservoir impoundment and experimental operation starting in 1983 [20].

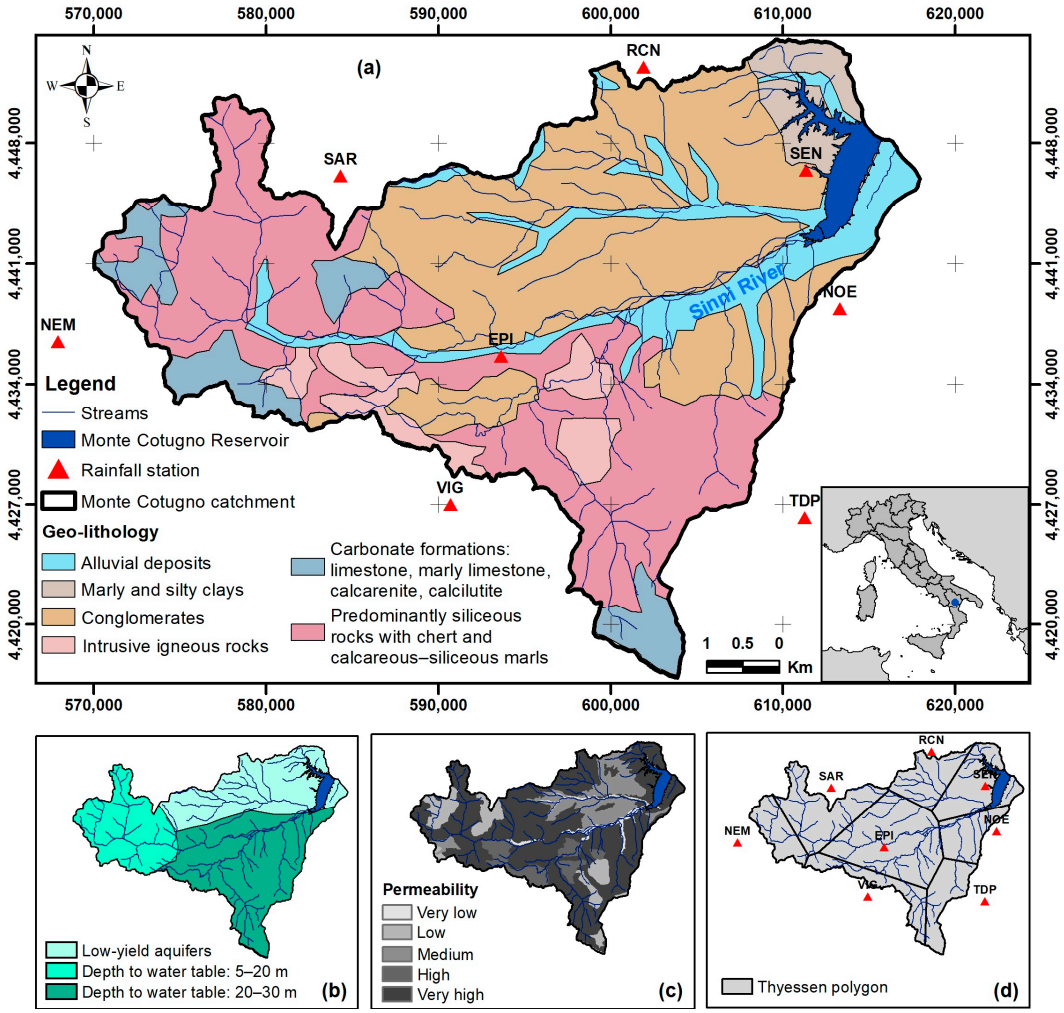

Figure 1. (**a**) Schematic geo-lithological map of the study area showing the location of the Monte Cotugno Reservoir and the rainfall stations used in this study. (**b**) Spatial distribution of aquifer depth across the catchment, distinguishing shallow and deep groundwater bodies. (**c**) Permeability map of the main lithological units, illustrating spatial variations in hydraulic conductivity across the basin. (**d**) Thiessen polygons used to compute area-weighted monthly precipitation based on the eight rainfall stations included in the analysis.

The reservoir represents the central node of the Ionico–Sinni water-distribution system, supplying irrigation, domestic, and industrial water to a wide region encompassing Basilicata, parts of Apulia, and the Metapontino plain, while also supporting the industrial district of Taranto.

The study area is dominated by sedimentary successions belonging to the Apenninic foredeep, with extensive Plio–Quaternary deposits. The prevailing lithologies include gray–blue marly clays and upper Pliocene calcareous marls, interlayered with sandy and sandy–gravel beds and, locally, thin conglomerate and sandstone horizons [21–23]. Up-

stream slopes and tributary valleys are partially mantled by alluvial, colluvial, and more recent unconsolidated deposits of generally limited thickness. The geological substrate underlying the Monte Cotugno dam consists of alternating units with marked permeability contrasts. Marls and clays act as effective aquitards, forming the main barriers to deep groundwater circulation, whereas sand and gravel layers are comparatively more permeable, although locally interrupted by cemented conglomeratic bodies. The dam foundation rests on a stratigraphic sequence in which near-surface sandy–gravel deposits of moderate permeability overlie much less permeable marly–clayey formations. This configuration exerts strong control on seepage processes, groundwater pathways, and the overall hydrological functioning of the reservoir.

The area exhibits hydroclimatic features typical of Mediterranean basins (Figure 2), with a progressive increase in both the intensity and frequency of sub-hourly and hourly extreme rainfall events, particularly during the summer and autumn seasons [24]. These short-duration storms are characterized by high erosive potential and contribute to an elevated susceptibility to rapid-onset hydrogeomorphological hazards, including flash floods, soil erosion and concentrated surface runoff [25].

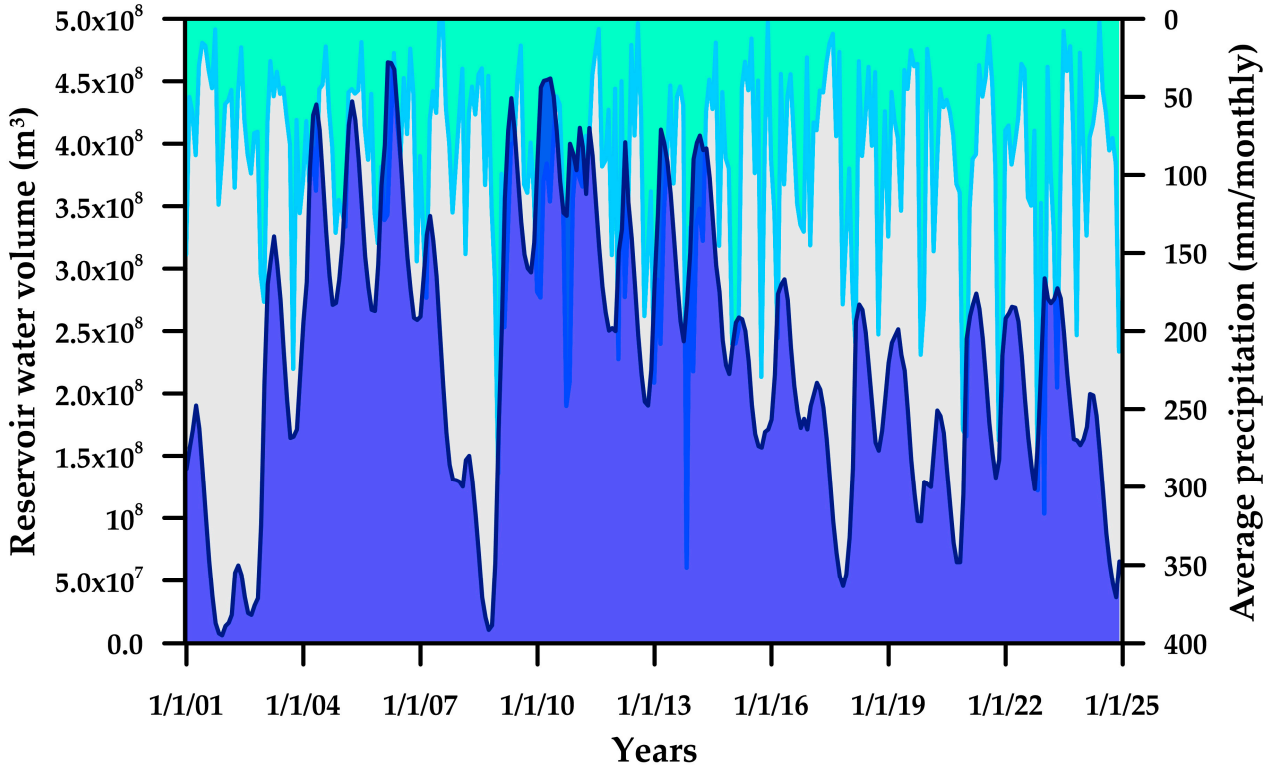

Figure 2. Time series of monthly reservoir water volume and basin-averaged precipitation for the Monte Cotugno reservoir, 2001–2024. The dark blue shaded area and line represent reservoir water volume (m^3), while the light blue line represents basin-averaged monthly precipitation (mm).

3. Materials and Methods

3.1. Datasets

Two primary datasets were used in this study. Monthly storage volumes for the Monte Cotugno Reservoir, covering the period 2001–2024, were obtained from the official basin authority website [20]. The reservoir volume dataset was examined for missing values, discontinuities and anomalous variations potentially attributable to operational adjustments or measurement errors. For consistency with the available hydrometeorological

information and to ensure homogeneous monitoring conditions, all subsequent analyses are therefore restricted to this 2001–2024 period.

Monthly precipitation records from eight meteorological stations (Table 1 and Figure 1a), located within or near the Sinni River basin that hosts the Monte Cotugno Reservoir, were retrieved from the regional hydrometeorological network (SI), i.e., the Hydrographic Service) and from the Servizio Agrometeorologico Lucano. These stations provide complete spatial coverage of the watershed and span the period January 2000–December 2024. All precipitation series were systematically screened for completeness and internal consistency.

Table 1. List of the eight rainfall stations used in this study for the Monte Cotugno basin. For each gauge mean rainfall over the period 2000–2024 and the corresponding Thiessen polygon weight contributing to the basin-average precipitation are reported.

Rainfall Station	Code	Elevation (m a.s.l.)	UTM Northing	UTM Easting	Mean Annual Rainfall (2000–2024)	Thiessen Weight
Castelsaraceno	SAR	850	4,455,838.137	575,650.278	1503.9	0.162
Episcopia	EPI	425	4,436,051.283	594,346.311	1117.4	0.267
Nemoli	NEM	450	4,436,461.735	567,932.222	1599.2	0.073
Noepoli	NOE	651	4,438,563.101	613,381.433	682.1	0.084
Roccanova	ROC	727	4,451,816.783	602,046.702	866.3	0.097
Senise	SEN	280	4,446,411.793	611,353.566	759.5	0.150
Terranova del Pollino	TDP	1232	4,426,713.094	610,759.067	967.3	0.086
Viggianello	VIG	550	4,423,230.144	588,601.366	1068.5	0.082

3.2. Standardized Reservoir Index

In this study, we used the Standardized Reservoir Index (SRI) [17], a drought indicator specifically developed to represent the combined effects of meteorological and anthropogenic influences on drought conditions using reservoir water-level (WL) data.

The SRI follows a procedure similar to that of the Standardized Precipitation Index (SPI), but differs in two key aspects:

1. The type of cumulative distribution function (CDF) is selected based on a goodness-of-fit test applied directly to the WL data, rather than assuming a predefined gamma distribution as in SPI.
2. The SPI constraint requiring the treatment or removal of zero values is not necessary, since WL data does not contain zeros.

A continuous time series of monthly reservoir storage volumes was first constructed. The Kolmogorov–Smirnov (K–S) goodness-of-fit test, applied at a significance level of 0.05, was then used to compare several candidate probability distributions for the storage data, including the gamma, log-normal, Weibull and generalized extreme value (GEV) distributions. For each distribution, K–S statistics and information criteria (AIC and BIC) were computed (Table 2). The Weibull distribution (Weibull_min) provides the best overall fit, yielding the smallest K–S statistic and the lowest AIC/BIC values; it was therefore adopted for SRI computation in this study.

The probability density function (PDF) of the Weibull distribution is defined as

$$f(v) = \frac{k}{\lambda}\left(\frac{v}{\lambda}\right)^{k-1} exp\left[-\left(\frac{v}{\lambda}\right)^{k}\right], \quad (1)$$

where v is the reservoir storage volume, $k > 0$ is the shape parameter and $\lambda > 0$ is the scale parameter. The support of the distribution is $v > 0$.

Table 2. Goodness-of-fit statistics for candidate probability distributions applied to monthly reservoir storage volumes at the Monte Cotugno reservoir (2001–2024). The table reports Kolmogorov–Smirnov (K–S) statistics and information criteria (AIC, BIC) for the gamma, log-normal, Weibull and generalized extreme value (GEV) distributions. The Weibull distribution shows the smallest K–S statistic and the lowest AIC/BIC values and is therefore adopted for SRI computation.

Distribution	K-S Statistic	AIC	BIC
Gamma	0.1051	11,557.7	11,568.6
Log-normal	0.1504	11,652.0	11,663.0
Weibull	0.0744	11,514.9	11,525.9
GEV	10.000	∞	∞

Once the Weibull distribution is fitted to the storage data, the cumulative probability for each monthly volume v_t is computed as

$$F(v_t) = 1 - exp\left[-\left(\frac{v_t}{\lambda}\right)^k\right]. \quad (2)$$

Finally, these cumulative probabilities are transformed into a standard normal variable, following the same standardization used for SPI:

$$\mathrm{SRI}_t = \Phi^{-1}(F(v_t)), \quad (3)$$

where $F(v_t)$ is the non-exceedance probability associated with storage v_t and Φ^{-1} is the inverse standard normal cumulative distribution function

3.3. Areal Precipitation Estimation and SPI Calculation

Eight rain gauges were selected based on their location within the catchment and the completeness of their records. Each station had to satisfy a preliminary quality-control criterion of less than 5% missing daily data over the 2000–2025 period. The eight daily series were then intercompared to identify and remove obvious outliers and inconsistencies. Missing values were subsequently reconstructed using linear regression with the most highly correlated neighboring stations, ensuring spatially coherent infilling. The quality-controlled daily precipitation series were then aggregated to monthly totals and catchment-scale areal monthly precipitation was finally estimated using the Thiessen polygon method [26], which assigns each station a weight proportional to the area of its associated Voronoi cell within the watershed (Figure 1d and Table 1). This analysis was performed in an ArcGIS 10.5 environment to ensure that station influence accurately matched watershed boundaries.

The resulting monthly areal precipitation series was used to compute the Standardized Precipitation Index (SPI) at 1-, 3-, 6-, and 12-month time scales. Following the standard methodology, cumulative precipitation at each scale was fitted to a gamma distribution and subsequently transformed to a standard normal distribution [27]. These SPI scales capture both short-term meteorological anomalies and longer-term hydrological deficits influencing reservoir inflows. SPI values were also computed individually for the eight rain gauges to evaluate their relationships with reservoir storage anomalies.

3.4. Trend Detection and Autocorrelation Treatment

Trend analysis of reservoir storage anomalies and SPI series was conducted using the non-parametric Mann–Kendall (MK) test [28,29], with Theil–Sen slope estimation used to quantify trend magnitude [30,31]. To mitigate bias arising from serial correlation a Trend-Free Prewhitening (TFPW) procedure was applied prior to MK testing [32,33]. Autocorrelation structure was quantified using lag-1 autocorrelation and partial autocorrelation

analyses. This combined approach provides robust identification of monotonic trends unaffected by hydrological memory. All statistical analyses were conducted in R (version 4.5.1) using the packages Kendall, trend and lmtest. While prewhitening ensures statistical robustness by controlling for autocorrelation, the raw series are also examined because, in the context of reservoir management, the persistence structure of storage anomalies is itself physically meaningful. This hydrological memory provides key information on the system's responsiveness and its capacity to buffer drought conditions, in line with the dual-approach recommended by previous studies [34–36].

3.5. Correlation and Lag Response Analysis

To assess the reservoir's response to hydroclimatic variability, Pearson [37] coefficients were computed between SPI values and normalized storage anomalies across multiple lag intervals. This multi-lag framework enables the identification of relevant response timescales and distinguishes between immediate and delayed hydrological responses to precipitation deficits or surpluses.

3.6. Causality Testing

To assess the directionality and potential causal links between the Standardized Precipitation Index (SPI, computed at multiple accumulation scales) and the reservoir storage anomaly (SV), Granger causality analysis [38] was performed in R (version 4.5.1) using the lmtest package. Following the classical framework, two nested autoregressive models were compared.

The univariate autoregressive model of order p is defined as:

$$Y_t = \sum_{m=1}^{p} a_m \, Y_{t-m} + \varepsilon_t \tag{4}$$

where Y_t denotes the target variable (SV), a_m are autoregressive coefficients, and ε_t is the residual error.

The full model additionally incorporates the lagged terms of the predictor series X_t (SPI):

$$Y_t = \sum_{m=1}^{p} a_m \, Y_{t-m} + \sum_{m=1}^{q} b_m \, X_{t-m} + \varepsilon_t \tag{5}$$

where b_m quantify the influence of past SPI values on SV dynamics.

The null hypothesis tested is:

$$H_0 : \; b_m = 0 \forall m$$

i.e., SPI does not Granger-cause SV. If the coefficients b_m are jointly significantly different from zero (F-test, $p < 0.05$), then past SPI values provide additional predictive information on SV beyond its own autoregressive structure.

A Vector Autoregressive model (VAR) was adopted, and the optimal lag order (lag = 2) was selected based on Akaike (AIC) and Bayesian Information Criteria (BIC). In addition to hypothesis testing, the strength of causality was quantified through the ratio of the residual variance of the restricted and full models (log-ratio), following the standard formulation in Granger causality literature.

Before fitting the VAR models, all-time series were assessed for stationarity using the Augmented Dickey–Fuller (ADF) test. Residual normality was evaluated using the Jarque–Bera test. When required, non-stationary series were differenced to meet the assumptions of VAR modeling.

4. Results

4.1. Evolution of the SRI and the Effect of Prewhitening

The monthly storage volume of the Monte Cotugno reservoir was standardized using the procedure described above, allowing direct comparison between reservoir anomalies and hydroclimatic indices. Over the study period, the Standardized Reservoir Index (SRI) exhibits a clear and systematically declining trajectory. Applying the Mann–Kendall (MK) test to the raw SRI series yields a Z-score of −3.979, coupled with a Theil–Sen slope of −0.00312, indicating a persistent and statistically significant negative trend (Table 3). This reveals a slow but continuous long-term depletion in standardized reservoir storage before any statistical correction.

Table 3. Mann–Kendall Z statistic, Autocorrelation (lag-1), pre-whitened MK Z and Theil–Sen slope for SRI and SPI indices (SPI1, SPI3, SPI6, SPI12) over the 2001–2024 period. MK = Mann–Kendall trend test; TFPW = Trend-Free Prewhitening applied.

Index	MK Z-Score	Sen's Slope	Autocorr. Lag-1	Autocorr. Significant	TFPW MK Z-Score	TFPW Sen's Slope
SRI	−3.979	−0.0031	0.951	Yes	−4.79	−0.00100
SPI1	1.489	0.0011	0.101	No	—	—
SPI3	3.237	0.0024	0.704	Yes	4.36	0.1071
SPI6	4.645	0.0035	0.861	Yes	8.89	0.0035
SPI12	6.707	0.0050	0.949	Yes	15.52	0.0050

The temporal structure of the SRI series is characterized by extraordinary persistence. Autocorrelation values remain extremely high for the first several lags (AC_1 = 0.951; AC_2 = 0.849; AC_3 = 0.712; AC_6 = 0.39; AC_{12} = 0.42), indicating that the reservoir retains memory for many months due to its large storage capacity, long residence time, and regulated inflow dynamics (Table 3). This level of persistence is considerably higher than that of any SPI scale, confirming that SRI represents a strongly smoothed hydrological signal primarily governed by long-term basin water balance conditions.

Such strong serial dependence (lag-1 autocorrelation ≈ 0.951) implies that the system is highly sensitive to past states, making prewhitening a necessary step for unbiased trend detection. After applying the Trend-Free Pre-Whitening (TFPW) procedure, the MK Z-score further decreases to −4.79, while the Sen's slope remains negative (−0.00100). The increase in MK significance following the removal of serial dependence confirms the intrinsic and robust nature of the declining trend. This demonstrates that the long-term depletion signal is not an artifact of autocorrelation but instead reflects a genuine hydrological degradation in reservoir storage conditions over the past two decades.

4.2. Trends and Persistence of SPI Indices (1–12 Months)

The temporal variability of the 1-, 3-, 6-, and 12-month Standardized Precipitation Index (SPI) provides a multi-scale perspective on hydroclimatic fluctuations in the Monte Cotugno basin. As summarized in Table 3, the joint evaluation of Mann–Kendall (MK) Z statistics, Trend-Free Prewhitening (TFPW) corrected values, Theil–Sen slopes and autocorrelation patterns allows a rigorous assessment of drought-index stationarity and persistence.

SPI1, which captures short-term moisture variability, exhibits very low autocorrelation across all lags (AC_1 = 0.101; AC_4 = 0.026; AC_6 = 0.035; AC_{12} = −0.030), indicating that monthly precipitation anomalies dissipate rapidly and are dominated by short-term atmospheric noise. The MK test on the raw series indicates a slight positive trend (Z = 1.4895; Sen's slope = 0.00109), showing that any observed increase is weak and easily obscured by internal variability.

SPI3, which represents short-to-intermediate moisture variability, displays more organized temporal behavior. Autocorrelations are significant at short lags (AC_1 = 0.7046; AC_2

= 0.378; AC_4 = 0.174; AC_6 = 0.189), and remain slightly positive up to lag 9 (AC_9 = 0.093). This intermediate memory reflects the influence of seasonal cycles, indicating that wet or dry conditions tend to persist for several consecutive months. The MK test on the raw series yields a positive trend (Z = 3.24), which remains detectable after TFPW (Z = 4.36), suggesting that the increasing tendency in SPI3 is not solely an artifact of serial correlation and likely reflects a genuine shift in multi-month precipitation conditions. Nevertheless, the Theil–Sen slopes (0.00237 raw; 0.0021 TFPW) indicate a moderate increase in 3-month accumulated precipitation.

SPI6, representative of sub-annual hydrological anomalies, exhibits strong and persistent autocorrelations (AC_1 = 0.861; AC_2 = 0.729; AC_3 = 0.622), with positive values extending to lag 12 (AC_{12} = 0.036). Such high persistence demonstrates that 6-month precipitation anomalies integrate previous events and remain influential over multiple months. The raw series shows a statistically significant positive trend (Z = 4.65; Sen's slope = 0.00351), which remains essentially unchanged after TFPW, confirming that the observed increase is robust and not an artifact of serial correlation.

SPI12, which integrates annual precipitation anomalies, displays the highest persistence of all indices, with extremely high autocorrelations at the first lags (AC_1 = 0.949; AC_2 = 0.894; AC_3 = 0.839) and remaining positive up to 12 months (AC_{12} = 0.250). This pattern is consistent with long-term hydroclimatic processes, including multi-year droughts or wet periods. The MK test indicates a strong positive annual trend (Z = 6.7069; Sen's slope = 0.005005), which remains virtually unchanged after TFPW, demonstrating that the long-term increase in normalized precipitation is statistically robust.

The combined analysis of trends and autocorrelation structures highlights that short-term indices (SPI1 and, to a lesser extent, SPI3) are dominated by high variability and low persistence, whereas longer-term indices (SPI6 and especially SPI12) exhibit strong memory and robust positive trends, confirming a progressively more pronounced increase in precipitation over the basin at intermediate and long timescales.

Overall, precipitation accumulated over 6–12 months shows a more consistent increase compared to shorter 1–3-month scales, with important implications for reservoir response and water resource dynamics in the Monte Cotugno basin.

4.3. Relationships Between SPI and SRI: Correlations and Causality

A crucial part of the analysis consists of investigating the extent to which SPI indices can explain or predict the behavior of the Standardized Reservoir Index (SRI). An initial visual inspection of the raw time series, where SPI and SRI are plotted together (Figure 3), reveals numerous interpretative nuances relevant for applied hydrology.

It is evident that SPI indices display a more "volatile" or intermittent component, characterized by sharp peaks and rapid fluctuations, which reflect short-term meteorological variability. In contrast, the SRI exhibits a smoothed, cumulative response, typical of reservoir-aquifer systems with significant water memory.

Specifically, periods are observed in which SPI temporarily returns to neutral or positive values, yet the SRI remains depressed for extended durations. This illustrates how drought events have persistent effects that are amplified in long-memory compartments. Conversely, when SPI values remain negative for several months, the SRI "collapses," reflecting the cumulative effect of precipitation deficits. Moreover, the correlation and coherence between SPI and SRI increase with longer SPI integration times, although the strength of this relationship is partly masked in the raw series by the strong persistence of reservoir storage.

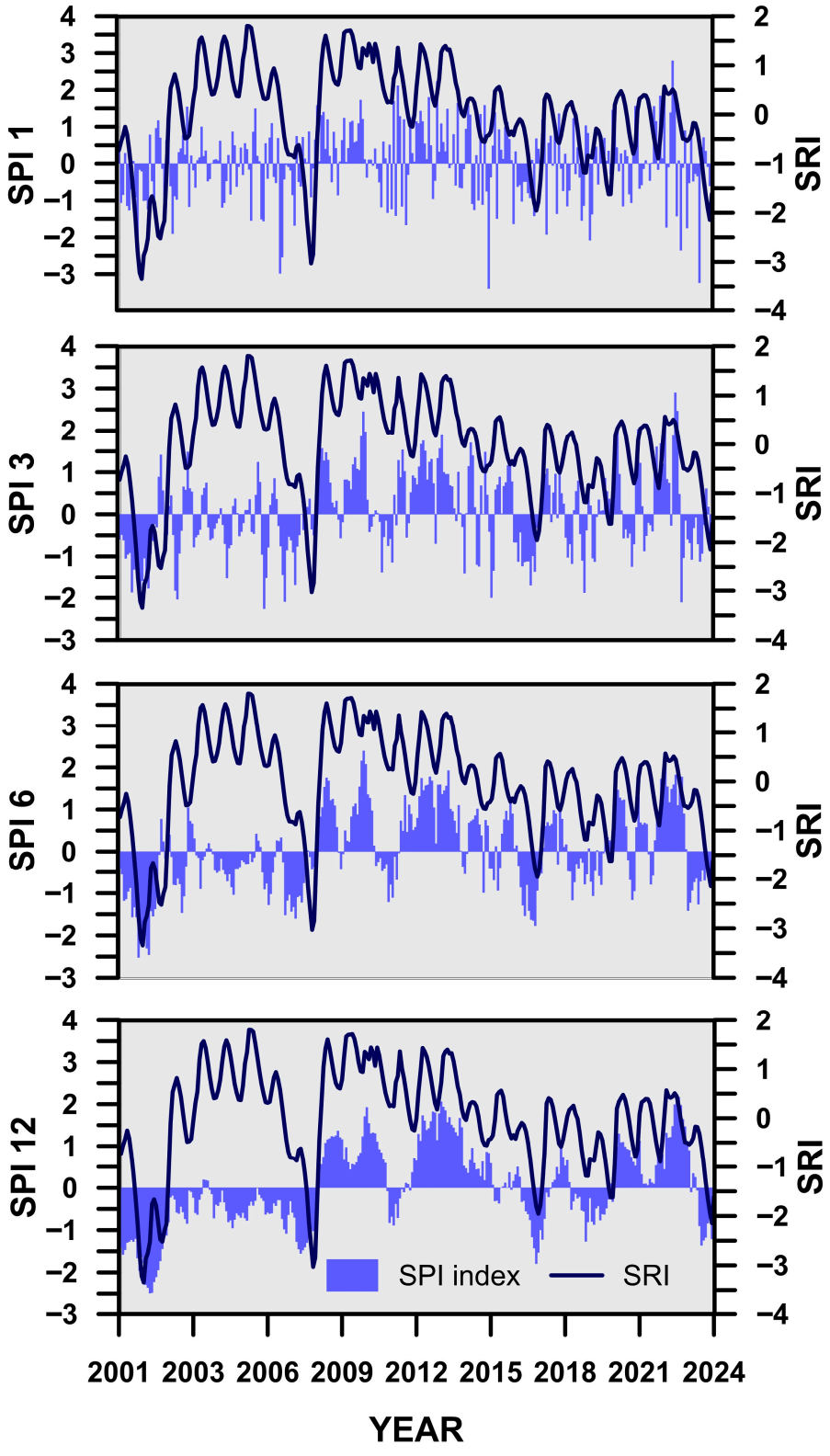

Figure 3. Time series of SPI and SRI for the Monte Cotugno reservoir at 1-, 3-, 6- and 12-month time scales over 2001–2024. In each panel, blue shaded bars represent the SPI, while the dark blue line represents the SRI.

Pearson correlations, Granger causality tests, and lagged cross-correlation analyses provide a quantitative framework to explore these relationships (Table 4).

Table 4. Pearson correlation coefficients and Granger causality tests between SRI and SPI indices (SPI1, SPI3, SPI6, SPI12), before and after TFPW correction (Monte Cotugno, 2001–2024). Statistical significance is indicated for each timescale.

Index	Pearson Corr. SRI	Pearson *p*-Value	Granger F	Granger *p*-Value	Granger Signif.	TFPW Pearson	TFPW *p*-Value	TFPW Granger F	TFPW Granger-p
SRI	—	—	—	—	—	—	—	—	—
SPI1	0.181	0.0021	0.53	0.587	No	0.258	9.0×10^{-6}	3.04	0.0495
SPI3	0.112	0.0581	2.51	0.0829	Marginal	0.197	0.00079	5.14	0.0064
SPI6	0.061	0.3005	0.72	0.4876	No	0.096	0.105	3.31	0.0379
SPI12	0.025	0.6674	2.45	0.0883	Marginal	0.006	0.922	6.26	0.0022

4.3.1. Pearson Correlations

For SPI1 vs. SRI, the Pearson correlation coefficient is approximately r = 0.18 with a significant *p*-value ($p \approx 0.002$), indicating a positive but weak relationship. For SPI3, the correlation remains modest ($r \approx 0.11$; $p \approx 0.06$), whereas SPI6 and SPI12 show only very weak and statistically non-significant correlations in the raw series ($r \approx 0.06$ and $r \approx 0.03$, respectively; $p > 0.30$). These results suggest that contemporaneous linear associations between monthly reservoir anomalies and SPI become less apparent in the presence of strong autocorrelation and shared low-frequency variability, and therefore need to be interpreted together with prewhitened and lagged metrics.

4.3.2. Granger Causality

When testing whether SPI1 "Granger-causes" SRI in the original (non-prewhitened) series at a lag of two months, the result is $F \approx 0.53$ with $p \approx 0.59$, indicating no statistically significant predictive power. For SPI3 vs. SRI, the F-statistic is about 2.51 ($p \approx 0.083$), and for SPI6 and SPI12 it is 0.72 ($p \approx 0.49$) and 2.45 ($p \approx 0.088$), respectively, again pointing to only marginal or non-significant causality in the raw data. Overall, these results indicate that, although reservoir storage and SPI share some common variability, the strong persistence of the SRI tends to obscure causal links in conventional Granger tests applied directly to the original series.

To better account for serial dependence, a Trend-Free Pre-Whitening (TFPW) procedure was applied to both SRI and SPI prior to the causality analysis. After TFPW, Pearson correlations increase and become statistically significant for SPI1 and SPI3, and Granger tests at a two-month lag indicate significant causality for all SPI scales (1–12 months), with *p*-values below 0.05. This behavior suggests that short- to long-term meteorological drought conditions exert a delayed but robust control on standardized reservoir storage, which becomes evident only after removing the masking effect of autocorrelation from both driver and response series.

4.3.3. Lagged Cross-Correlation

Complementing the trend and causality analyses, a lagged cross-correlation between SPI indices and SRI was performed, using both raw and TFPW-corrected series, to quantify the time delay with which precipitation anomalies propagate to the reservoir (Figure 4). In the non-prewhitened (raw) series, the maximum correlation coefficient increases with SPI time scale: SPI1 ($r \approx 0.27$, lag -6), SPI3 ($r \approx 0.39$, lag -5), SPI6 ($r \approx 0.49$, lag -4), and SPI12 ($r \approx 0.59$, lag 0), indicating that the reservoir response time shortens as precipitation deficits are accumulated over longer integration periods. After applying TFPW, SPI–SRI cross-correlations are generally reduced in magnitude and become more localized in time, reflecting the removal of shared low-frequency persistence between meteorological forcing and reservoir storage. In this prewhitened framework, cross-correlations highlight the "instantaneous" component of the linkage that remains after accounting for long-term mem-

ory and are consistent with the significant Pearson and Granger relationships identified in the previous subsection.

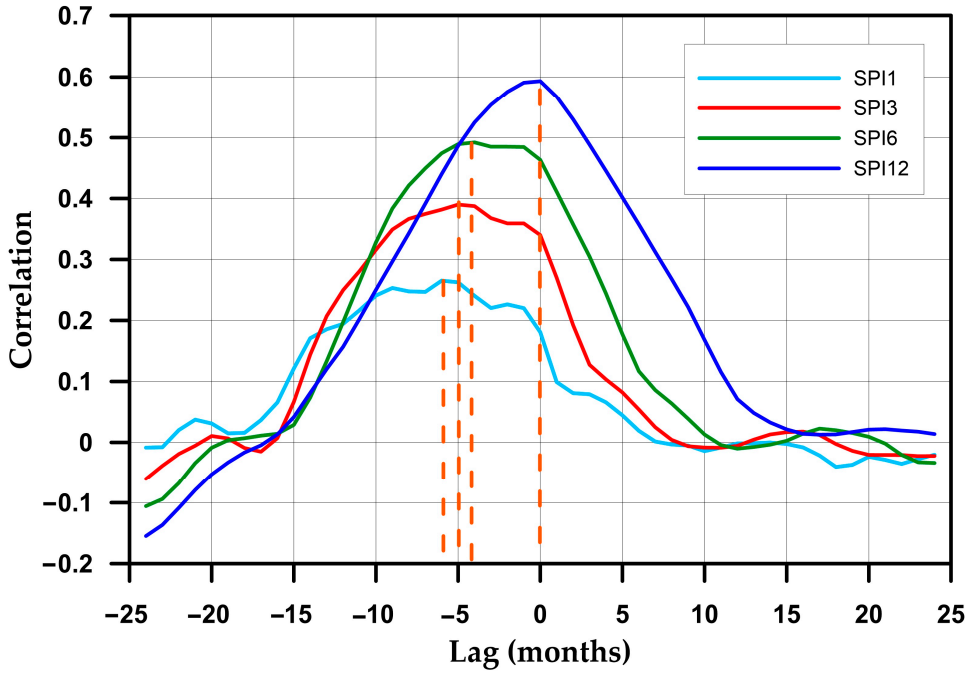

Figure 4. Lagged cross-correlation functions between SPI indices and SRI.

It should be noted that, in practical hydrological applications, TFPW may underestimate the apparent strength of the functional dependence between SPI (meteorological forcing) and SRI (reservoir response), particularly in operational and predictive contexts, where the full effect of persistence is often exploited. Therefore, the analysis of raw data remains useful for applied purposes, whereas TFPW-based diagnostics provide a more conservative but less biased estimate of the underlying statistical linkages.

These results demonstrate that the reservoir responds more slowly to short-term precipitation anomalies, whereas SRI and SPI become increasingly synchronized as drought conditions persist over longer time scales, consistent with the hydrological memory of the basin and the cumulative nature of reservoir storage.

5. Discussion

The analysis of the Monte Cotugno reservoir highlights the interplay between hydroclimatic variability, represented by the Standardized Precipitation Index (SPI) and reservoir storage dynamics expressed by the Standardized Reservoir Index (SRI). Over the 2001–2024 period, the SRI exhibits a persistent decline. Mann–Kendall testing on the raw SRI series confirms a statistically significant downward trend, which remains robust after applying TFPW, indicating that the negative trajectory is not merely an artifact of serial correlation but a genuine feature of reservoir behavior.

The high lag-1 autocorrelation of the SRI demonstrates the strong hydrological memory of the system, whereby past storage levels substantially influence current volumes, and autocorrelations remain notable even at longer lags, reflecting persistence throughout the year [39–41].

SPI indices provide complementary insight into the multi-scale variability of hydroclimatic conditions in the basin. Short-term anomalies (SPI1) display low persistence and negligible trends, while intermediate scales (SPI3 and SPI6) exhibit stronger autocorrelations and more pronounced trends. Annual-scale SPI12 demonstrates the highest

persistence and largest trend magnitude. These patterns indicate that short-term precipitation variability alone has limited impact on reservoir storage, whereas multi-month and annual anomalies accumulate sufficiently to influence SRI, highlighting the importance of considering multiple temporal scales for assessing hydrological response [42,43].

The relationship between SPI and SRI strengthens with increasing timescale. In the raw series, contemporaneous Pearson correlations increase from weak to moderate values as the SPI accumulation period lengthens, with the highest coefficient for SPI12. After applying TFPW to both SRI and SPI, correlations become statistically significant at short to intermediate scales (SPI1–SPI3), and Granger causality tests at a two-month lag indicate significant predictive power for all SPI scales, confirming that meteorological drought at 1–12-month timescales exert a delayed but robust control on standardized reservoir storage. Lagged cross-correlation analysis further demonstrates that short-duration anomalies precede SRI changes by several months, whereas longer-duration anomalies are nearly synchronous with the reservoir response; in the raw series, the maximum correlation coefficient increases with SPI scale, from about $r \approx 0.27$ at a lag of roughly -6 months for SPI1 to $r \approx 0.59$ at lag 0 for SPI12, indicating that the reservoir response time shortens as precipitation deficits are accumulated over longer integration periods. This behavior reflects the reservoir's hydrological memory: short precipitation anomalies must persist or accumulate to affect storage, while longer anomalies are more directly and rapidly reflected in SRI [40].

An explanation for the sometimes weak and non-stationary relationship between SPI and reservoir storage lies in the role of groundwater resources and baseflow contributions. Historically, during dry periods or phases of intense water demand, groundwater abstractions and sustained baseflow have buffered surface water deficits, allowing reservoir storage to remain relatively high even under negative precipitation anomalies. However, long-term overexploitation and insufficient recharge have progressively depleted aquifer storage in many aquifers of southern Italy, including parts of Basilicata. Regional studies document declining net rainfall, reduced groundwater recharge and increasing groundwater drought conditions under recent climate variability [44–46]. Regional assessments for Basilicata [47] highlight that recent reductions in autumn–winter precipitation have simultaneously limited surface-water availability and groundwater replenishment, increasing pressure on multi-reservoir systems and inter-basin transfers. These conditions support the plausibility of a groundwater-mediated attenuation of runoff response in the study area. Under current conditions, a substantial portion of precipitation is first required to restore groundwater levels before contributing to effective surface runoff and reservoir inflow. As a consequence, even periods characterized by positive SPI values may not translate into corresponding increases in reservoir storage, resulting in persistently low SRI values despite increasing rainfall. This behavior is clearly visible in several multi-month episodes during the 2000s and 2010s, including phases around 2005–2006, 2012–2013 and 2015–2016, where SPI3–SPI12 return to near-normal or moderately wet conditions (SPI > 0) while SRI remains negative or shows only a weak recovery, as illustrated in Figure 3, indicating that reservoir storage continues to reflect antecedent deficits despite improving precipitation anomalies. Although piezometric data were not available for direct analysis, this interpretation is strongly supported by analogous evidence from Mediterranean basins affected by long-term groundwater depletion and drought dynamics assessed through multi-index approaches [48,49].

Nevertheless, the hydroclimatic patterns must also be interpreted in the context of the current water management challenges in Basilicata, where system losses are extraordinarily high. Official data from ISTAT and regional reports indicate that in 2022–2023 the total water loss in the Basilicata distribution network reached 65.5%, the highest in Italy [50,51].

In absolute terms, approximately 115 billion liters of potable water were lost over the last three years, reflecting a systemic inefficiency in both urban and irrigation networks. Potenza, the regional capital, exhibits the worst performance with 71% of water lost, while other main centers maintain losses above 63% [52].

The temporal trend is also alarming: losses have increased by nearly 8 percentage points over recent years, consistently exceeding the national average of 42.4% [53]. Although recent initiatives (2023–2025) have produced partial improvements in certain areas, the critical situation remains widespread. The losses affect not only urban water supply but also agricultural irrigation networks managed by Consorzio di Bonifica, where obsolete infrastructure and inefficient management amplify water wastage. This has profound economic and environmental implications, negatively impacting local agriculture, export potential, and the sustainability of intensive crops, particularly in the Metapontino area [54,55].

Adding another layer of complexity, structural integrity issues at Monte Cotugno may also play a role in limiting effective storage. Geophysical studies have revealed localized infiltration zones within the dam [56], indicating potential conduits for water movement into and through the structure. Although such infiltration has not been fully quantified as an operational "loss" in volumetric terms, its presence underscores the system's vulnerability. Geotechnical and long-term monitoring investigations at Monte Cotugno further confirm the presence of localized defects in the diaphragm and foundation sealing system, with seepage discharges collected in the inspection tunnels on the order of a few liters per second and peaks slightly above 10 L s^{-1} during high reservoir levels, while the embankment remains essentially dry and the overall efficiency of the sealing system is maintained. These results indicate that seepage pathways exist and contribute to the structural vulnerability of the dam–foundation system, but they also suggest that, at least over the monitored period, seepage volumes are relatively limited compared to the total reservoir capacity and cannot be isolated as a dominant driver of the long-term decline in SRI [57].

Integrating hydroclimatic and operational data reveals that multi-month and annual precipitation deficits are not fully mitigated by the reservoir system, which already suffers from extremely high distribution losses. In this study, information on water losses is therefore used to document the macro-scale infrastructural inefficiency that constrains the translation of stored water into effective supply, while the observed SRI decline is interpreted as the result of combined hydroclimatic deficits, groundwater stress and structural/operational inefficiencies, whose individual contributions cannot yet be statistically disentangled. Even where SPI indicates sufficient rainfall, the SRI reflects lower storage levels due to the combined effects of climatic stress, groundwater depletion, structural constraints and systemic inefficiencies in the conveyance network. The degree of alignment between SPI and SRI at longer timescales is therefore strongly influenced by the structural and operational conditions of the water distribution network, highlighting the need to combine climate-based monitoring with proactive infrastructure management [58–61].

Overall, the results indicate that the Basilicata water system is under dual pressure: natural climatic variability and persistent anthropogenic losses. While intermediate and long SPI indices are valuable for predicting reservoir storage, the practical capacity to buffer droughts is severely constrained by the macro-scale inefficiency of the network, making water conservation and infrastructure improvement urgent priorities.

6. Conclusions

The Monte Cotugno reservoir illustrates the dual pressures increasingly faced by Mediterranean water systems: persistent hydroclimatic variability and chronic anthropogenic inefficiency. Statistical analyses conducted over more than two decades reveal

a clear and significant downward trend in standardized reservoir storage (SRI), primarily driven by cumulative operational losses, persistent human-induced pressures, and longstanding infrastructure limitations. This negative trajectory cannot be attributed to a progressive reduction in precipitation, as SPI indices at seasonal and annual timescales remain largely stationary or even show slight positive tendencies.

Although multi-month and annual SPI indices provide reliable predictors of storage variability, the reservoir's practical ability to buffer drought conditions is severely constrained by outdated infrastructure, distribution network losses, and insufficient operational flexibility. The pronounced hydrological memory detected through autocorrelation and trend analyses further underscores the system's limited resilience to recurring dry spells and management shortcomings. In particular, the demonstrated predictive power of SPI3 and SPI6 for SRI variations suggests that short-to-medium-term SPI anomalies could be operationally used as early-warning indicators: when SPI3–SPI6 fall below predefined drought thresholds, reservoir operating rules could be tightened (for example by reducing releases and increasing seasonal storage targets), whereas positive SPI phases could be exploited to rebuild storage in anticipation of subsequent droughts.

Overall, the findings emphasize the need for advanced water-management strategies that integrate multi-scale hydroclimatic forecasting, rigorous statistical monitoring, explicitly accounting for serial dependence and urgent improvements in infrastructure and governance. In practical terms, modernization efforts should prioritize the rehabilitation of the most inefficient segments of the urban and irrigation distribution networks, where loss rates are persistently highest, and the strengthening of the operational capacity of irrigation consortia, ensuring adequate staffing and technical functionality so that SPI-informed reservoir management and water-saving strategies effectively translate into reduced losses and more efficient use of water resources in the Basilicata region and, more broadly, across Mediterranean reservoir systems facing similar challenges.

Author Contributions: Conceptualization. M.P. and M.B.; methodology. M.P.; software. M.P.; validation. M.P.; formal analysis. M.P.; investigation. M.P.; resources. M.P.; data curation. M.P.; writing—original draft preparation. M.P.; writing—review and editing. M.P. and M.B.; visualization. M.P. and M.B.; supervision. M.B.; project administration. M.B.; funding acquisition. M.B. All authors have read and agreed to the published version of the manuscript.

Funding: This research was funded by the Italian Ministry of University and Research (MUR) through the PRIN PNRR project "Origin and evolution of insular large mammals from the central Mediterranean area—OMEGA" (project code P2022RZ4PL, CUP C53D23007210001), granted to MarioBentivenga (Università della Basilicata).

Data Availability Statement: Historical reservoir storage data for the Monte Cotugno Reservoir (monthly net volumes for the period 1998–2025) are publicly available from the Autorità di Bacino Distrettuale dell'Appennino Meridionale website (http://www.adb.basilicata.it/adb/risorseidriche/dispoidriche/ScegliDatiDighe.asp?maxData=20260113, accessed on 11 January 2026), which provides graphical access to the time series for the main Lucanian reservoirs (Monte Cotugno, San Giuliano, Pertusillo). Basin precipitation data were obtained from the regional hydrometeorological network (Servizio Idrografico) and from the Servizio Agrometeorologico Lucano; these datasets can be requested via the contacts indicated on the respective institutional websites. Derived, non-sensitive products generated in this study (monthly SPI and SRI series and basic descriptive statistics) are available from the corresponding author upon request.

Acknowledgments: The authors thank the Academic Editor and the three anonymous reviewers for their constructive comments and suggestions, which helped to improve the clarity and robustness of the manuscript.

Conflicts of Interest: The authors declare no conflicts of interest.

Abbreviations

The following abbreviations are used in this manuscript:

SRI Standardized Resorvoir Index
SPI Standardized Precipitation Index

References

1. Palatnik, R.R.; Raviv, O.; Sirota, J.; Shechter, M. Water scarcity and food security in the mediterranean region: The role of alternative water sources and controlled-environment agriculture. *Water Resour. Econ.* **2025**, *49*, 100256. [CrossRef]
2. MedECC. *Climate and Environmental Change in the Mediterranean Basin—Current Situation and Risks for the Future*; First Mediterranean Assessment Report (MAR1); Union for the Mediterranean, Plan Bleu, UNEP/MAP: Marseille, France, 2020; ISBN 978-2-9577416-0-1. Available online: https://www.medecc.org/medecc-reports/climate-and-environmental-change-in-the-mediterranean-basin-current-situation-and-risks-for-the-future-1st-mediterranean-assessment-report/ (accessed on 1 December 2025).
3. IEMed; Plan Bleu. *Water Challenges in the Mediterranean*; IEMed Mediterranean Yearbook 2021; European Institute of the Mediterranean: Barcelona, Spain, 2021; Available online: https://www.iemed.org/publication/water-challenges-in-the-mediterranean (accessed on 1 December 2025).
4. Seker, M.; Gumus, V. Projection of temperature and precipitation in the Mediterranean region through multi-model ensemble from CMIP6. *Atmos. Res.* **2022**, *280*, 106440. [CrossRef]
5. Silvestri, L.; Saraceni, M.; Brunone, B.; Meniconi, S.; Passadore, G.; Bongioannini Cerlini, P. Assessment of seasonal soil moisture forecasts over the Central Mediterranean. *Hydrol. Earth Syst. Sci.* **2025**, *29*, 925–946. [CrossRef]
6. Vicente-Serrano, S.M.; Tramblay, Y.; Reig, F.; González-Hidalgo, J.C.; Beguería, S.; Brunetti, M.; Kalin, K.C.; Patalen, L.; Kržič, A.; Lionello, P.; et al. High temporal variability not trend dominates Mediterranean precipitation. *Nat. Commun.* **2025**, *639*, 658–666. [CrossRef] [PubMed]
7. Ingrao, C.; Strippoli, R.; Lagioia, G.; Huisingh, D. Water scarcity in agriculture: An overview of causes, impacts and approaches for reducing the risks. *Heliyon* **2023**, *9*, e18507. [CrossRef]
8. Macias, D.; Bisselink, B.; Carmona-Moreno, C.; Druon, J.-N.; Duteil, O.; Garcia-Gorriz, E.; Grizzetti, B.; Guillen, J.; Miladinova, S.; Pistocchi, A.; et al. The overlooked impacts of freshwater scarcity on oceans as evidenced by the Mediterranean Sea. *Nat. Commun.* **2025**, *16*, 998. [CrossRef]
9. Navarro-Ortega, A.; Acuña, V.; Bellin, A.; Burek, P.; Cassiani, G.; Choukr-Allah, R.; Dolédec, S.; Elosegi, A.; Ferrari, F.; Ginebreda, A.; et al. Managing the effects of multiple stressors on aquatic ecosystems under water scarcity: The GLOBAQUA project. *Sci. Total Environ.* **2015**, *503–504*, 3–9. [CrossRef]
10. Zaniolo, M.; Giuliani, M.; Sinclair, S.; Burlando, P.; Castelletti, A. When timing matters—Misdesigned dam filling impacts hydropower sustainability. *Nat. Commun.* **2021**, *12*, 3056. [CrossRef]
11. Hou, J.; van Dijk, A.I.J.M.; Beck, H.E.; Renzullo, L.J.; Wada, Y. Remotely sensed reservoir water storage dynamics (1984–2015) and the influence of climate variability and management at a global scale. *Hydrol. Earth Syst. Sci.* **2022**, *26*, 3785–3803. [CrossRef]
12. Wang, Z.; Jiang, L.; Nielsen, K.; Wang, L. Reservoir filling up problems in a changing climate: Insights from CryoSat2 altimetry. *Geophys. Res. Lett.* **2024**, *51*, e2024GL108934. [CrossRef]
13. Baba, W.M.; Chehbouni, A.; Ouassanouan, Y.; Gascoin, S.; Paganini, M.; Ottavianelli, G.; Szantoi, Z. Monitoring water crisis from space across a Mediterranean region. *Sci. Rep.* **2025**, *15*, 23262. [CrossRef]
14. Vicente-Serrano, S.M.; López-Moreno, J.I. Hydrological response to different time scales of climatological drought: An evaluation of the Standardized Precipitation Index in a mountainous Mediterranean basin. *Hydrol. Earth Syst. Sci.* **2005**, *9*, 523–533. [CrossRef]
15. Chen, H.; Xu, B.; Qiu, H.; Huang, S.; Teegavarapu, R.S.V.; Xu, Y.-P.; Guo, Y.; Nie, H.; Xie, H. Adaptive assessment of reservoir scheduling to hydrometeorological comprehensive dry and wet condition evolution in a multi-reservoir region of southeastern China. *J. Hydrol.* **2024**, *634*, 132392. [CrossRef]
16. Montaldo, N.; Sirigu, S.; Zucca, R.; Ruiu, A.; Corona, R. Hydrological Sustainability of Dam-BasedWater Resources in a Mediterranean Basin Undergoing Climate Change. *Hydrology* **2024**, *11*, 200. [CrossRef]
17. Sadeghfam, S.; Farmani, H.; Mirabbasi, R. Developing reservoir drought index and conducting copula-based frequency analysis for Lake Urmia basin in Iran. *J. Hydrol. Reg. Stud.* **2025**, *60*, 102476. [CrossRef]
18. Von Storch, H.; Navarra, A. *Analysis of Climate Variability—Applications of Statistical Techniques*; Springer: New York, NY, USA, 1995.

19. Costigliola, R.M.; Mancuso, C.; Pagano, L.; Silvestri, F. Seismic safety evaluation of an existing bituminous faced rockfill dam. In *Earthquake Geotechnical Engineering for Protection and Development of Environment and Constructions, Proceedings of the 7th International Conference on Earthquake Geotechnical Engineering (ICEGE), Rome, Italy, 17–20 June 2019*; Silvestri, F., Moraci, N., Eds.; CRC Press: Boca Raton, FL, USA; Taylor & Francis Group: Abingdon, UK, 2019; pp. 1887–1893. ISBN 978-0-367-14328-2.
20. Available online: http://www.adb.basilicata.it/adb/risorseidriche/dispoidriche/ScegliDatiDighe.asp?maxData=20260113 (accessed on 15 October 2025).
21. ISPRA. Carta Geologica d'Italia Alla Scala 1:50.000 Foglio 522 Senise. Istituto Superiore per la Protezione e la Ricerca Ambientale, Servizio Geologico d'Italia 2011. Available online: https://www.isprambiente.gov.it/Media/carg/522_SENISE/Foglio.html (accessed on 22 November 2025).
22. Giannandrea, P.; Loiacono, F. Le successioni alluvionali e lacustri quaternarie affioranti nella media valle del Fiume Sinni (Appennino meridionale, Basilicata). *Il Quat.* **2003**, *16*, 257–267.
23. Giano, S.; Giannandrea, P. Late Pleistocene differential uplift inferred from the analysis of fluvial terraces (southern Apennines, Italy). *Geomorphology* **2014**, *217*, 89–105. [CrossRef]
24. Piccarreta, M.; Bentivenga, M.; Piccarreta, R. Trend Analysis of Hourly Rainfall in the Mediterranean: A Case Study of the Basilicata Region, Southern Italy (2001–2024). *Theor. Appl. Climatol.* **2026**, *157*, 10. [CrossRef]
25. Piccarreta, M.; Lazzari, M.; Bentivenga, M. The influence in rainfall erosivity calculation by using different temporal resolution in Mediterranean area. *Sci. Total Environ.* **2024**, *906*, 167411. [CrossRef]
26. Bayraktar, H.; Turalioglu, F.; Şen, Z. The estimation of average areal rainfall by percentage weighting polygon method in Southeastern Anatolia Region, Turkey. *Atmos. Res.* **2005**, *73*, 149–160. [CrossRef]
27. McKee, T.B.; Doesken, N.J.; Kleist, J. The relationship of drought frequency and duration to time scales. In Proceedings of the 8th Conference on Applied Climatology, Anaheim, CA, USA, 17–22 January 1993; pp. 179–184.
28. Kendall, M.G. *Rank Correlation Methods*; Griffin: Oxford, UK, 1948.
29. Mann, H.B. Nonparametric tests against trend. *Econometrica* **1945**, *13*, 245–259. [CrossRef]
30. Sen, P.K. Estimates of the regression coefficient based on Kendall's tau. *J. Am. Stat. Assoc.* **1968**, *63*, 1379–1389. [CrossRef]
31. Theil, H. A rank-invariant method of linear and polynomial regression analysis. *Proc. R. Neth. Acad. Sci.* **1950**, *53*, 386–392 521–525 1397–1412.
32. Yue, S.; Pilon, P.; Phinney, B.; Cavadias, G. The influence of autocorrelation on the ability to detect trend in hydrological series. *Hydrol. Process* **2002**, *16*, 1807–1829. [CrossRef]
33. Yue, S.; Wang, C.Y. Applicability of prewhitening to eliminate the influence of serial correlation on the Mann–Kendall test. *Water Resour. Res.* **2002**, *38*, 1068. [CrossRef]
34. Serinaldi, F.; Kilsby, C.G. The importance of prewhitening in change point analysis under persistence. *Stoch. Environ. Res. Risk Assess.* **2016**, *30*, 763–777. [CrossRef]
35. Khanal, S.; Lutz, A.F.; Immerzeel, W.W.; Vries, H.d.; Wanders, N.; Hurk, B.v.d. The Impact of Meteorological and Hydrological Memory on Compound Peak Flows in the Rhine River Basin. *Atmosphere* **2019**, *10*, 171. [CrossRef]
36. Serinaldi, F. Scientific logic and spatio-temporal dependence in analyzing extreme-precipitation frequency: Negligible or neglected? *Hydrol. Earth Syst. Sci.* **2024**, *28*, 2987–3016. [CrossRef]
37. Pearson, K. Notes on Regression and Inheritance in the Case of Two Parents. *Proc. R. Soc. Lond.* **1895**, *58*, 240–242. [CrossRef]
38. Granger, C.W.J. Investigating Causal Relations by Econometric Models and Cross-spectral Methods. *Econometrica* **1969**, *37*, 424–438. [CrossRef]
39. Hulsman, P.; Hrachowitz, M.; Savenije, H.H.G. Improving the representation of long-term storage variations with conceptual hydrological models in data-scarce regions. *Water Resour. Res.* **2021**, *57*, e2020WR028837. [CrossRef]
40. Van Loon, A.F.; Kchouk, S.; Matanó, A.; Tootoonchi, F.; Alvarez-Garreton, C.; Hassaballah, K.E.A.; Wu, M.; Wens, M.L.K.; Shyrokaya, A.; Ridolfi, E.; et al. Review article: Drought as a continuum—Memory effects in interlinked hydrological, ecological, and social systems. *Nat. Hazards Earth Syst. Sci.* **2024**, *24*, 3173–3205. [CrossRef]
41. Wang, X.; Tu, X.; Peng, T.; Singh, V.P.; Zhou, Z.; Lin, K. Analysis of drought propagation from meteorological to hydrological drought under the impact of a super-large reservoir. *J. Hydrol. Reg. Stud.* **2025**, *62*, 102801. [CrossRef]
42. Chaves, H.M.L.; da Silva, C.C.; Fonseca, M.R.S. Reservoir Reliability as Affected by Climate Change and Strategies for Adaptation. *Water* **2023**, *15*, 2323. [CrossRef]
43. Ji, R.; Wang, C.; Cui, A.; Wang, W.; Chen, N. Separating climate and human induced terrestrial water storage anomalies with GRACE data and hydrological models. *Int. J. Digit. Earth* **2025**, *18*, 2557516. [CrossRef]
44. Mendicino, G.; Senatore, A.; Versace, P. A Groundwater Resource Index (GRI) for drought monitoring and forecasting in a mediterranean climate. *J. Hydrol.* **2008**, *357*, 282–302. [CrossRef]
45. De Vita, P.; Allocca, V.; Celico, F.; Fabbrocino, S.; Cesaria, M.; Monacelli, G.; Musilli, I.; Piscopo, V.; Scalise, A.R.; Summa, G.; et al. Hydrogeology of continental southern Italy. *J. Maps* **2018**, *14*, 230–241. [CrossRef]

46. Lepore, D.; Bucchignani, E.; Montesarchio, M.; Allocca, V.; Coda, S.; Cusano, D.; De Vita, P. Impact scenarios on groundwater availability of southern Italy by joint application of regional climate models (RCMs) and meteorological time series. *Sci. Rep.* **2024**, *14*, 20337. [CrossRef]
47. Polemio, M.; Casarano, D. Climatic change, drought and groundwater availability in southern Italy. In *Climate Change and Groundwater; Special Publication*; Dragoni, W., Ed.; Geological Society: London, UK, 2008; Volume 288, pp. 39–51.
48. Henao Casas, J.D.; Fernández Escalante, E.; Ayuga, F. Alleviating drought and water scarcity in the Mediterranean region through managed aquifer recharge. *Hydrogeol. J.* **2022**, *30*, 1685–1699. [CrossRef]
49. Elsaidy, A.; Villani, L.; Yimer, E.A.; Gómez, M.M.; Huysmans, M.; Mogheir, Y.; van Griensven, A. Groundwater drought assessment in a Mediterranean coastal catchment through a multi-index approach. *J. Hydrol. Reg. Stud.* **2026**, *63*, 103043. [CrossRef]
50. Available online: https://www.istat.it/it/archivio/282919 (accessed on 1 December 2025).
51. Available online: https://statscom.regione.basilicata.it/perdite-idriche-in-basilicata-al-62/ (accessed on 1 December 2025).
52. Available online: https://blue-community.net/2025/01/12/water-emergency-in-italys-basilicata (accessed on 1 December 2025).
53. Available online: https://www.anbi.it/art/news/9189-siccita-in-puglia-e-basilicata-in-crisi-anche-il-servizio-po (accessed on 1 December 2025).
54. Available online: https://www.basilicata24.it/2025/09/agricoltura-a-secco-nel-metapontino-continua-il-disservizio-irriguo-del-consorzio-di-bonifica-152558/ (accessed on 1 December 2025).
55. Canora, F.; Muzzillo, R.; Sdao, F. Groundwater Vulnerability Assessment in the Metaponto Coastal Plain (Basilicata, Italy). *Water* **2022**, *14*, 1851. [CrossRef]
56. Loperte, A.; Soldovieri, F.; Palombo, A.; Santini, F.; Lapenna, V. An integrated geophysical approach for water infiltration detection and characterization at Monte Cotugno rock-fill dam (southern Italy). *Eng. Geol.* **2016**, *211*, 162–170. [CrossRef]
57. Callari, C.; Jappelli, R. Comportamento a breve e a lungo termine della diga di Monte Cotugno sul fiume Sinni. In Proceedings of the Atti del XXII Convegno Nazionale di Geotecnica, Palermo, Italy, 22–24 September 2004; pp. 469–477, ISBN 978-8855527705.
58. Saase, R.; Schütt, B.; Bebermeier, W. Analyzing the Dependence of Major Tanks in the Headwaters of the Aruvi Aru Catchment on Precipitation. Applying Drought Indices to Meteorological and Hydrological Data. *Water* **2020**, *12*, 2941. [CrossRef]
59. Bahrami, N.; Nikoo, M.R.; Al-Rawas, G.; Al-Wardy, M.; Gandomi, A.H. Reservoir optimal operation with an integrated approach for managing floods and droughts using NSGA-III and prospect behavioral theory. *J. Hydrol.* **2022**, *610*, 127961. [CrossRef]
60. Thomaz, F.R.; Miguez, M.G.; de Souza Ribeiro de Sá, J.G.; de Moura Alberto, G.W.; Fontes, J.P.M. Water Scarcity Risk Index: A Tool for Strategic Drought Risk Management. *Water* **2023**, *15*, 255. [CrossRef]
61. Guo, Y.; Liu, L. Reservoir Control Operations and Water Resources Management. *Water* **2024**, *16*, 3000. [CrossRef]